



Magnetogenesis by Wave-driven Momentum Exchange

Ian E. Ochs and Nathaniel J. Fisch

Department of Astrophysical Sciences, Princeton University, Princeton, NJ 08540, USA; iochs@princeton.edu
Received 2020 August 7; revised 2020 September 30; accepted 2020 October 25; published 2020 December 8

Abstract

When multiple species interact with an electrostatic ion acoustic wave, they can exchange momentum, despite the lack of momentum in the field itself. The resulting force on the electrons can have a curl, and thus give rise to compensating electric fields with curl on magnetohydrodynamic timescales. As a result, a magnetic field can be generated. Surprisingly, in some astrophysical settings, this mechanism can seed magnetic fields with growth rates even larger than through the traditional Biermann battery.

Unified Astronomy Thesaurus concepts: [Astrophysical magnetism \(102\)](#); [Cosmic magnetic fields theory \(321\)](#); [Galaxy magnetic fields \(604\)](#); [Primordial magnetic fields \(1294\)](#); [Plasma physics \(2089\)](#); [Plasma astrophysics \(1261\)](#); [Interstellar magnetic fields \(845\)](#)

1. Introduction

Explaining the magnetic field structures present on different astrophysical scales is very difficult. The observed magnetic fields in the universe are thought to be largely the result of amplification of small fields by magnetic dynamo mechanisms (Schober 2011; Brandenburg et al. 2012; Squire & Bhattacharjee 2015; St-Onge et al. 2020). However, the dynamo requires a small, preexisting “seed” magnetic field to act upon. The generation of these seed fields on different scales is an area of active research.

Various mechanisms have been proposed as origins of these seed fields, from the Weibel instability (Schlickeiser & Shukla 2003), to currents from charged cosmic rays (Miniati & Bell 2011; Ohira 2020), to expulsion by jets from magnetized compact objects (Daly & Loeb 1990), to photon pressure on charged particles (Munirov & Fisch 2019). However, the dominant favored mechanism in most scenarios (Kulsrud et al. 1997; Gnedin et al. 2000; Hanayama et al. 2005; Hanayama & Tomisaka 2006; Naoz & Narayan 2013; Zweibel 2013) is the Biermann battery (Schlüter & Biermann 1950; Ridgers et al. 2020). The basic insight behind the mechanism is that electrons, with their negligible mass relative to ions, are inertia-free on magnetohydrodynamic (MHD) timescales. Hence, the electrons must always be in force balance, and so a direct current (DC) electric field must arise that cancels all other forces on the electrons. If the applied non-DC force-per-electron F_e/n_e has curl, the induced electric field will also have curl, and give rise to a magnetic field via Faraday’s law.

For the Biermann battery, the relevant force density is the pressure gradient, and a field is produced when the temperature and density gradients are misaligned. Such nonaligned temperature and density gradients can be produced by shock-induced turbulence in the plasma, which can occur for instance when the expanding bubble of a supernova impacts an inhomogeneous interstellar medium (ISM; Hanayama et al. 2005; Hanayama & Tomisaka 2006).

Although the Biermann battery and literature that invokes it focuses on large-scale pressure forces, this is not the only force that can lead to Biermann-like magnetic induction. In particular, we examine the forces resulting from wave-particle interactions. Theory (Moiseev & Sagdeev 1963; Chen 1984)

and experiments (Taylor et al. 1970) show that shocks in an unmagnetized plasma form structures with trailing Debye-scale ion acoustic waves (IAWs). Thus, the same astrophysical shocked systems (Eichler 1979; Hanayama et al. 2005) that give rise to Biermann generation are likely to give rise to IAWs and their associated forces. Although the IAW, as an oscillating pressure force, does not lead to averaged Biermann field generation, as an electrostatic wave it can mediate directed momentum exchange between the electrons and ions along the direction of the wavevector (Ochs & Fisch 2020). Thus, the IAW provides a net force on the electrons that, like the pressure gradient force in the Biermann mechanism, can have curl, and thus produce a magnetic field on MHD timescales. As we show here, in some circumstances this mechanism, which we term the “IAW battery,” could lead to faster field growth than the Biermann battery.

2. Biermann Battery from a Force with Curl

The Biermann battery effect can be derived from Maxwell’s equations and the electron momentum equation:

$$\frac{\partial \mathbf{B}}{\partial t} = -c \nabla \times \mathbf{E}, \quad (1)$$

$$m_e n_e \frac{d\mathbf{v}_e}{dt} = -en_e \left(\mathbf{E} + \frac{\mathbf{v}_e}{c} \times \mathbf{B} \right) + \mathbf{F}_e. \quad (2)$$

Here, we use Gaussian units, \mathbf{F}_e represents the force density due to all other forces on the electrons, and the remaining notation is standard. To take the MHD limit, we consider a timescale long enough for the force on the electrons to equilibrate, which is equivalent to taking $m_e \rightarrow 0$. This makes Equation (2) an algebraic rather than differential equation, which we solve for \mathbf{E} :

$$\mathbf{E} = -\frac{\mathbf{v}_e}{c} \times \mathbf{B} + \frac{\mathbf{F}_e}{en_e}. \quad (3)$$

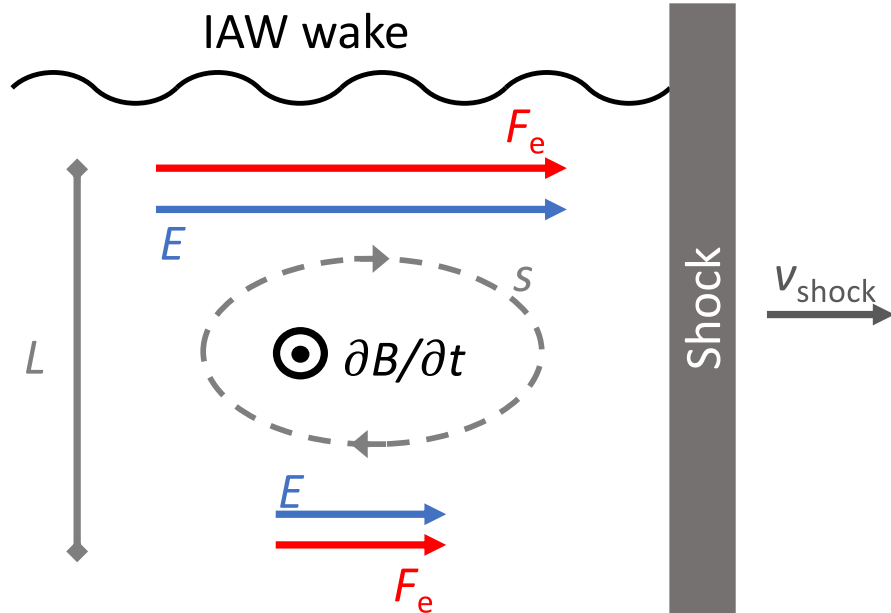


Figure 1. Mechanism of magnetogenesis by ion acoustic waves. A shock propagates through the ISM, producing ion acoustic waves in its wake. These waves produce force F_e electrons, inhomogeneous on a scale L in the ISM. A compensating inhomogeneous electric field E arises to cancel this force. This field has curl (consider the integral of the field over the loop s), and thus induces a magnetic field B .

This is the Ohm's law for our MHD model. Taking $v_e \approx v_i \equiv v$ and plugging Equation (3) into Equation (1) then yields

$$\frac{\partial \mathbf{B}}{\partial t} = \nabla \times (\mathbf{v} \times \mathbf{B}) - \frac{c}{e} \nabla \times \left(\frac{\mathbf{F}_e}{n_e} \right). \quad (4)$$

For the Biermann battery, the relevant force is the electron pressure gradient force, $\mathbf{F}_e = -\nabla(n_e T_e)$. Plugging this in to Equation (4) yields the Biermann battery:

$$\frac{\partial \mathbf{B}}{\partial t} \Big|_{\text{Bier}} = \frac{c}{en_e} \nabla n_e \times \nabla T_e. \quad (5)$$

In a typical astrophysical scenario, a shock will nonadiabatically heat the inhomogeneous ISM, leading to nonaligned density and pressure gradients. For instance, the supernova explosion of a primordial star results in an expanding shock around the supernova remnant (SNR; Miranda et al. 1998; Hanayama et al. 2005). The growth rate of the field can then be estimated as

$$\frac{\partial B}{\partial t} \Big|_{\text{Bier}} \approx \frac{c T_e}{e L^2} \sin \theta, \quad (6)$$

where θ is the typical angle between the density and temperature gradients, and the scale length L associated with the Biermann battery is the inhomogeneity scale length in the ISM, approximately 1–10 pc.

3. IAW Battery

Shocks do not only form nonaligned pressure and density gradients: they can also produce IAWs in the plasma (Moiseev & Sagdeev 1963; Taylor et al. 1970; Chen 1984). Thus, it is important to examine the effect of such waves on the generation of magnetic fields.

The electric field associated with a purely electrostatic plane wave such as an IAW has no momentum. Therefore, if the wave interacts with only one species, it cannot apply a net force as it damps. However, a wave interacting with multiple species *can* provide a net force to each species individually, as long as the forces on all species sum to zero.

An IAW in a plasma flattens the velocity distribution function in the neighborhood of the sound speed $C_s \equiv \sqrt{(ZT_e + T_i)/m_i}$, where Z and m_i are the ion charge state and mass, respectively. Because there tend to be more particles at low energy, the net effect is to accelerate particles to higher energy and momentum along the phase velocity. This energy transfer from the wave into the particles is known as Landau damping. To conserve momentum, the damping wave shifts the nonresonant velocity distribution in the opposite direction. For an IAW, most of this nonresonant momentum transfer goes into the ions, so that both the electron and ion distributions experience a net force due to the wave.

The momentum transfer rate to the electrons for a narrow IAW spectrum with $ZT_e \gg T_i$ is given by Ochs & Fisch (2020):

$$\mathbf{F}_e \approx \sqrt{\frac{\pi}{2}} \sqrt{\frac{Zm_e}{m_i}} \mathcal{W} \mathbf{k}, \quad (7)$$

where \mathcal{W} is the energy in the IAW (including the oscillating kinetic energy of the particles) and \mathbf{k} is the wavevector.

Inhomogeneities in a shocked plasma will naturally lead to inhomogeneities in the wave spectrum generated by the shock, and so can produce an \mathbf{F}_e with curl. As in the Biermann battery, the resulting electron force will be compensated by an electric field with curl, and thus induce a magnetic field (Figure 1). According to Equation (4), and using the result from geometric optics for a narrow spectrum that $\nabla \times \mathbf{k} = 0$ (Dodin &

Fisch 2012), the field growth rate will be

$$\frac{\partial \mathbf{B}}{\partial t}|_{\text{IAW}} = -\frac{c}{e} \sqrt{\frac{\pi Z m_e}{2 m_i}} \nabla \left(\frac{\mathcal{W}}{n_e} \right) \times \mathbf{k}. \quad (8)$$

Thus, the scaling of the IAW battery is

$$\frac{\partial \mathbf{B}}{\partial t}|_{\text{IAW}} \approx \frac{c}{e} \sqrt{\frac{\pi Z m_e}{2 m_i}} \frac{\mathcal{W} k}{n_e L}. \quad (9)$$

We can get the ratio of the Biermann growth rate to the IAW growth rate simply by dividing Equation (9) by Equation (6). Recalling that $k = 2\pi/\lambda_{\text{IAW}}$, where λ_{IAW} is the typical wavelength of an IAW, we arrive at our estimate of the relative strengths:

$$\frac{\partial \mathbf{B}/\partial t|_{\text{IAW}}}{\partial \mathbf{B}/\partial t|_{\text{Bier}}} \sim \left(\frac{\sqrt{2\pi^3}}{\sin \theta} \sqrt{\frac{Z m_e}{m_i}} \right) \left(\frac{\mathcal{W}}{P_e} \right) \left(\frac{L}{\lambda_{\text{IAW}}} \right). \quad (10)$$

Here, the first factor is $\mathcal{O}(10^{-1})$ at $\sin \theta = 1$, and can be significantly larger if the Biermann-relevant temperature and density gradients are closely aligned. The second factor is $\mathcal{O}(1)$, if the wave energy is in equipartition with the thermal energy. The final factor is the number of IAW wavelengths on a correlation scale. There seems to be a great deal of uncertainty around the wavelength of shock-trailing IAWs in astrophysical settings, which could range from the experimentally consistent electron Debye length, i.e., 160 m for the 100 eV plasma at 0.2 cm^{-3} typical of the shock-heated ISM that could be found around a primordial SNR (McKee & Ostriker 1977; Hanayama et al. 2005), to the scale of several parsecs (Spitzer 1982). Thus, the last term could be extremely large, and so it is quite plausible for the IAW growth rate to dominate in some scenarios.

4. Connection to Current Drive in Laboratory Plasmas

An advantage of the IAW magnetogenesis mechanism is that the wave field itself need not carry any momentum, since it can drive current by catalyzing the exchange of momentum between electrons and ions. It is worthwhile to note that magnetogenesis by waves that themselves carry no momentum has been recognized both in theory and laboratory plasma experiments (Fisch 1987). For example, the electron cyclotron wave induces asymmetric collisions between electrons and ions (Fisch & Boozer 1980) to drive current.

In the case of laboratory settings, magnetogenesis by waves has generally been termed “current drive,” or “radio-frequency (RF) current drive.” This nomenclature arises, perhaps, because of the emphasis on maintaining steady-state currents and their associated steady-state magnetic fields in laboratory devices, rather than on the ab initio generation of the magnetic field. This steady state is maintained by the constant injection of RF wave power, which is balanced by collisional (resistive) dissipation of the current. However, the very same waves that maintain the steady state can, of course, also be used to generate the magnetic field. Thus, lower hybrid waves can maintain steady-state currents (Fisch 1978), but can also quite spectacularly generate large magnetic fields as well (Fisch & Karney 1985).

These RF current drive mechanisms, in an initial-value problem for the generation of the field, would enter in Equation (4) through a force on electrons that is not curl free,

much in the same way as the Biermann battery term or the IAW battery term enters. This approach accounts for the self-induction of the plasma that opposes the creation of the field, but that does not play a role in the eventual steady state. For the case of RF current drive, the field reaches a saturated steady state when the force term is balanced by collisional or resistive terms that do not appear in the collisionless limit of Ohm’s law as presented in Equation (3). If resistivity is neglected, then other physical effects must be included to describe the saturation of the magnetogenesis, as described in the next section.

5. Saturation

A large growth rate is not sufficient to establish the IAW battery as a seeding mechanism for astrophysical magnetic fields. As the battery proceeds, the plasma structure changes, and at some point the mechanism will saturate and the field production will cease. For the mechanism to be viable, the saturation level of the fields must be high enough to seed the astrophysical dynamo mechanisms—on the order of 10^{-20} – 10^{-16} G for galactic magnetic fields (Widrow 2002).

The first possible method of saturation, for either the Biermann battery or IAW battery, is the complete relaxation of the driving force. For the Biermann battery, the pressure gradient should relax on approximately the sound crossing time L/C_s . Thus, integrating Equation (6) over this time, and taking $ZT_e \gg T_i$, we find

$$B_{\text{max,Bier}} \approx \frac{cm_i C_s}{eL} \sin \theta. \quad (11)$$

This condition can be expressed more cleanly in terms of the ion cyclotron frequency $\Omega_{i,\text{Bier}} \equiv eB_{\text{max,Bier}}/cm_e$ associated with the saturated field, and the sound crossing time L/C_s across the ISM scale length:

$$\Omega_{i,\text{Bier}} \left(\frac{L}{C_s} \right) \lesssim \sin \theta. \quad (12)$$

This expression assumes that the pressure force is thermal, rather than ram pressure; otherwise, the right-hand side will get an extra factor of $P_{\text{ram}}/n_e T_e$.

For the IAW battery, the driving force stops when the wave completely damps. Integrating Equation (9) over time, and using the results for a general wave that $\partial \mathcal{W}/\partial t = 2\omega_i \mathcal{W}$, where for an electron-damped IAW $\omega_i = -|\omega| \sqrt{\pi/8} \sqrt{Z m_e/m_i}$, we find a similar result to that for the Biermann battery:

$$\Omega_{i,\text{IAW}} \left(\frac{L}{C_s} \right) \lesssim \frac{\mathcal{W}}{P_e}. \quad (13)$$

Thus, the ratio of the magnetic field saturation level in the Biermann versus IAW battery is equal to the ratio of wave to thermal energy in the plasma.

However, for the IAW battery, there is a second saturation mechanism due to feedback from the magnetic field. As the field grows in a plane perpendicular to \mathbf{k} , it will begin to influence the wave, preventing electron motion along \mathbf{k} . The wave–particle interaction will be significantly impacted when the electron cyclotron frequency Ω_e becomes comparable to the wave frequency $\omega = C_s k$. Thus, in addition to the constraint on the ion cyclotron frequency, we have a constraint on the

electron cyclotron frequency:

$$\Omega_{e,\text{IAW}} \left(\frac{\lambda_{\text{IAW}}}{2\pi C_s} \right) \lesssim 1. \quad (14)$$

These constraints can be combined as

$$\Omega_{i,\text{IAW}} \left(\frac{L}{C_s} \right) \lesssim \min \left(\frac{\mathcal{W}}{P_e}, \frac{Zm_e}{m_i} \frac{2\pi L}{\lambda_{\text{IAW}}} \right). \quad (15)$$

Thus, comparing to Equation (12), we see that there should be many IAW wavelengths within the characteristic gradient scale length for the IAW battery to saturate at a similar level as the Biermann battery.

Finally, we can express the saturation field in number form, which becomes

$$B_{\text{IAW}} \lesssim \begin{cases} 3.31 \times 10^{-17} \sqrt{\frac{\mu}{Z}} \frac{\mathcal{W}}{P_e} \left(\frac{T_e}{1 \text{ eV}} \right)^{1/2} \left(\frac{L}{1 \text{ pc}} \right)^{-1} \text{ G} \\ 1.13 \times 10^{-19} \sqrt{\frac{Z}{\mu}} \left(\frac{T_e}{1 \text{ eV}} \right)^{1/2} \left(\frac{\lambda_{\text{IAW}}}{1 \text{ pc}} \right)^{-1} \text{ G}, \end{cases} \quad (16)$$

where μ is the ion mass in a.m.u. Thus, around a primordial SNR, short-wavelength (relative to the ISM inhomogeneity scale length of ~ 1 pc) IAWs in a shock-heated (~ 100 eV) ISM could be able to seed galactic fields even at the level of 10^{-16} G. As the wavelength becomes shorter and the hydrodynamic energy larger, the battery grows even stronger.

6. Discussion

There are some subtleties and caveats associated with the IAW battery. In this section, we discuss in more detail the assumptions that go into the model, as well as their applicability.

First, an acoustic wave is formed by a set of oscillating pressure gradients, and yet we have demanded that the pressure gradient scale length L be much greater than the acoustic wavelength λ_{IAW} . This is consistent, however, because the IAW field is oscillating; the resulting pressure force (and thus Biermann generation) will oscillate also, tending to cancel or at most grow as a random walk, $B \propto \sqrt{t}$. The corresponding IAW battery field, however, grows linearly with time. Thus, the ion acoustic wavelength is a relevant scale length for the IAW field, but not the Biermann field.

Second, the IAW battery requires that IAWs be only weakly damped by ions, i.e., $ZT_e \gg T_i$. Thus, there must be either a source of electron heating, or some high charge states present in the plasma.

Third, the electron force term in Equation (7) is for a narrow spectrum of waves. However, farther from the shock, the wave spectrum is likely to become turbulent, consisting of many wavenumbers pointing in many different directions. The net force on the electrons will then result from some average of the forces from these different wavenumbers. As long as there is an overall anisotropy that remains in the wavenumber distribution, resulting from the symmetry breaking from the shock propagation, the IAW battery will continue to operate, but total isotropization of the wave spectrum will kill the battery.

Fourth, the electron force term in Equation (7) applies to a Maxwellian plasma. However, as the force is applied, the velocity distribution function will flatten in the neighborhood of the resonance, weakening the force. The wave spectrum broadening discussed in the previous paragraph will

significantly mitigate this flattening, by bringing more parts of the electron distribution into resonance. Then, collisions between electrons must balance the remaining flattening for a force to continue to be applied. However, collisions between electrons and ions will add resistivity to the plasma, relaxing the generated field. Thus, there must be enough collisions to keep the distribution function approximately Maxwellian near resonance, but not so many that the field diffuses out. This is likely to be the case in the shock-heated ISM, where the collision time is on the order of years to decades for $(n, T) \sim (10^{-2} \text{ cm}^{-3}, 10^2 \text{ eV})$ (McKee & Ostriker 1977), while the dynamical timescales for, e.g., the expansion of an SNR are on the order of 10^5 yr (Hanayama et al. 2005).

Finally, the growth rate of this mechanism must of course be compared to other wave-driven mechanisms for any specific scenario. For instance, the strong oscillations of the electric potential in the immediate wake of an unmagnetized shock can lead to strong anisotropy in the electron velocity distribution, seeding the Weibel instability (Schlickeiser & Shukla 2003; Medvedev et al. 2006; Stockem et al. 2014). This mechanism is not exactly colocated with the IAW battery, which is likely to operate further downstream, where the acoustic waves have smaller amplitude and electron trapping only occurs immediately around resonance. However, it is difficult to say which mechanism dominates in the long-time limit, as the IAW battery (like the Biermann battery) produces a linearly growing large-scale field, while the Weibel instability produces an exponentially growing small-scale field, which is then subject to nonlinear processes such as dynamo amplification and possibly reconnection. Schoeffler et al. (2014) have used particle-in-cell simulations to study the conditions under which Biermann versus Weibel magnetic generation mechanisms tend to be dominant, and found that the Weibel instability tends to dominate in large systems. It seems plausible that the IAW battery dominance will resemble the Biermann dominance due to their similar underlying mechanisms and scaling, but a detailed study of the interplay between the IAW battery and the Weibel instability requires further study.

7. Conclusion

We showed how wave-driven momentum exchange could provide a magnetogenesis mechanism similar to the Biermann battery in astrophysical settings, and how this mechanism could potentially be stronger than the Biermann mechanism in certain scenarios. Unusually, it is a kinetic mechanism that produces fields on hydrodynamic length scales. As a mechanism that is based on long-established, experimentally verified plasma physics models, the IAW battery is an attractive candidate for magnetogenesis in astrophysical settings.

We would like to thank E. J. Kolmes and M. E. Mlodik for helpful discussions. This work was supported by grants DOE DE-SC0016072 and DOE NNSA DE-NA0003871. I.E.O. also acknowledges the support of the DOE Computational Science Graduate Fellowship (DOE grant No. DE-FG02-97ER25308).

ORCID iDs

Ian E. Ochs  <https://orcid.org/0000-0002-6002-9169>

Nathaniel J. Fisch  <https://orcid.org/0000-0002-0301-7380>

References

- Brandenburg, A., Sokoloff, D., & Subramanian, K. 2012, *SSRv*, **169**, 123
- Chen, F. F. 1984, *Introduction to Plasma Physics*, Vol. 1 (2nd ed.; New York: Plenum)
- Daly, R., & Loeb, A. 1990, *ApJ*, **364**, 451
- Dodin, I. Y., & Fisch, N. J. 2012, *PhRvA*, **86**, 53834
- Eichler, D. 1979, *ApJ*, **229**, 419
- Fisch, N. J. 1978, *PhRvL*, **41**, 873
- Fisch, N. J. 1987, *RvMP*, **59**, 175
- Fisch, N. J., & Boozer, A. H. 1980, *PhRvL*, **45**, 720
- Fisch, N. J., & Karney, C. F. 1985, *PhRvL*, **54**, 897
- Gnedin, N. Y., Ferrara, A., & Zweibel, E. G. 2000, *ApJ*, **539**, 505
- Hanayama, H., Takahashi, K., Kotake, K., et al. 2005, *ApJ*, **633**, 941
- Hanayama, H., & Tomisaka, K. 2006, *ApJ*, **641**, 905
- Kulsrud, R. M., Cen, R., Ostriker, J. P., & Ryu, D. 1997, *ApJ*, **480**, 481
- McKee, C., & Ostriker, J. 1977, *ApJ*, **218**, 148
- Medvedev, M. V., Silva, L. O., & Kamionkowski, M. 2006, *ApJL*, **642**, L1
- Miniati, F., & Bell, A. R. 2011, *ApJ*, **729**, 73
- Miranda, O. D., Opher, M., & Opher, R. 1998, *MNRAS*, **301**, 547
- Moiseev, S. S., & Sagdeev, R. Z. 1963, *JNuE*, **5**, 43
- Munirov, V. R., & Fisch, N. J. 2019, *PhRvE*, **100**, 023202
- Naoz, S., & Narayan, R. 2013, *PhRvL*, **111**, 051303
- Ochs, I. E., & Fisch, N. J. 2020, *PhPI*, **27**, 062109
- Ohira, Y. 2020, *ApJL*, **896**, L12
- Ridgers, C. P., Arran, C., Bissell, J. J., & Kingham, R. J. 2020, arXiv:2009.01562
- Schlickeiser, R., & Shukla, P. K. 2003, *ApJL*, **599**, L57
- Schlüter, A., & Biermann, L. 1950, *ZNatA*, **5**, 237
- Schober, J. 2011, PhD thesis, Univ. Heidelberg <https://www.ita.uni-heidelberg.de/~jschober/Diplomarbeit.pdf>
- Schoeffler, K. M., Loureiro, N. F., Fonseca, R. A., & Silva, L. O. 2014, *PhRvL*, **112**, 175001
- Spitzer, L., Jr. 1982, *ApJ*, **262**, 315
- Squire, J., & Bhattacharjee, A. 2015, *PhRvL*, **115**, 175003
- St-Onge, D. A., Kunz, M. W., Squire, J., & Schekochihin, A. A. 2020, *JPIPh*, **86**, 905860503
- Stockem, A., Grismayer, T., Fonseca, R. A., & Silva, L. O. 2014, *PhRvL*, **113**, 105002
- Taylor, R. J., Baker, D. R., & Ikezi, H. 1970, *PhRvL*, **24**, 206
- Widrow, L. M. 2002, *RvMP*, **74**, 775
- Zweibel, E. 2013, *PhyOJ*, **6**, 85